Journal of Intelligent Systems and Control
https://www.acadlore.com/journals/JISC

# Enhanced Control of Dual Star Induction Motor via Super Twisting Algorithm: A Comparative Analysis with Classical PI Controllers

Es-saadi Terfia[1*], Sofiane Mendaci[2], Salah Eddine Rezgui[3], Hamza Gasmi[4], Walid Kantas[1]

[1] Laboratory of Electrical Engineering of Guelma (LGEG), Department of Electrotechnical and Automatic Engineering, Université 8 Mai 1945 Guelma, 24000 Guelma, Algeria
[2] Laboratoire d'Automatique et Informatique de Guelma (LAIG), Department of Electrical Engineering, Université 8 Mai 1945 Guelma, 24000 Guelma, Algeria
[3] Laboratory of Electrotechnics of Constantine, Department of Electrical Engineering, Engineer Sciences Faculty, Frères Mentouri Constantine 1 University, 25000 Constantine, Algeria
[4] Laboratoire de Contrôle Avancé (LABCAV), Department of Electronic and Télécommunication, Université 8 Mai 1945 Guelma, 24000 Guelma, Algeria

[*] Correspondence: Es-saadi Terfia (terfia.es-saadi@univ-guelma.dz)

**Received:** 10-12-2023 **Revised:** 11-20-2023 **Accepted:** 12-10-2023

**Citation:** E. Terfia, S. Mendaci, S. E. Rezgui, H. Gasmi, and W. Kantas, "Enhanced control of dual star induction motor via super twisting algorithm: A comparative analysis with classical PI controllers," *J. Intell Syst. Control*, vol. 2, no. 4, pp. 220–229, 2023. https://doi.org/10.56578/jisc020404.



**Abstract:** In the field of industrial motor control, the inherent design complexity and operational challenge of dual star induction motor (DSIM) have made it a focus of research for many scholars. This study attempts to innovatively propose a refined control approach for DSIM, by deploying two pulse width modulation (PWM) voltage sources combining with indirect field-oriented control (IFOC). Core of our innovation is the integration of a super twisting algorithm (STA) controller, which is a strategy specifically designed to enhance the motor's speed control capability. The paper introduced the technical details of DSIM, with the focus placed on the distinctive configuration of two isolated neutral three-phase windings, set apart by a 30-degree electrical phase shift. Such design has posed certain control challenges, and the STA approach has skillfully addressed these challenges. With the help of Matlab/Simulink simulations, the efficacy of STA controller is evaluated and compared with the common Proportional-Integral (PI) controller, and the simulation results are indicative of the STA controller's superiority, showing a significant improvement in reducing torque ripples and stator current fluctuations. The analysis given in the paper quantifies the improvement, showing substantial reductions in steady-state error and response time, as well as an enhanced disturbance rejection capability. These findings are instrumental in showcasing the STA controller's comparative advantage. Concludingly, the adoption of the STA-based control methodology in DSIM applications not only fosters enhanced speed control and efficiency but also holds the promise of broad applicability across various industrial scenarios. This research, therefore, marks a pivotal advancement in the field of DSIM control, potentially revolutionizing its application in diverse industrial settings. The consistency in the use of professional terminology throughout the paper ensures a coherent and comprehensive understanding of the subject matter.

**Keywords:** Dual star induction motor (DSIM); Indirect field-oriented control (IFOC); Pulse width modulation (PWM); Super twisting algorithm (STA); Control systems

## 1 Introduction

Electric variable-speed drives have become the backbone of modern industrial systems, enabling precise control over motor functions. Among the various control methods, field-oriented control (FOC) stands out for its ability to emulate the independent control achieved in DC motors by ensuring a decoupling control between flux and torque [1, 2]. This study attempts to cope with these challenges and propose potential solutions within the realm of FOC, focusing on its application in DSIM.

The inherent variability of motor parameters is a major challenge for achieving optimal control effectiveness [3]. Although the three-phase asynchronous machines are the mainstream in application, the multi-phase machines, especially DSIMs, are now a compelling alternative for high-power systems [4, 5]. DSIM has two windings with

isolated neutrals, spatially phase-displaced by $\alpha = 30$ electrical degrees [6, 7]. To realize variable speed drive for DSIM, two PWM voltage sources, controlled by the IFOC strategy, are used to supply these windings.

However, the control effectiveness of IFOC for DSIMs faces challenges due to variations in the machine's rotor resistance and other motor parameters [8]. Traditional PI controllers, commonly employed in such scenarios, exhibit weaknesses in rejecting external disturbances and are sensitive to changes in system parameters [8–11].

To address these challenges, we introduce a nonlinear control technique that leverages the STA as an alternative to conventional PI controllers within the IFOC strategy. STA, known for its robustness in handling complex and non-linear processes, offers a promising solution [12, 13]. Unlike conventional controllers, STA remains unaffected by changes in parameter values, enhancing its reliability and efficiency [14, 15].

Objective of this study is to enhance the benefits of the IFOC strategy for DSIMs by introducing the STA-based control method. The proposed approach seeks to significantly improve speed control performance, reduce torque ripples, and minimize stator current undulations. The technical description of DSIM is simplified to underscore its unique design challenges, particularly the 30-degree electrical phase shift between the isolated neutral three-phase windings.

To validate the efficacy of the proposed STA-based control method, we conduct comparative Matlab/Simulink simulations. These simulations compare the performance of the STA controller against the conventional PI controller, emphasizing improvements in steady-state error, disturbance rejection, and response time. The results highlight the comparative nature of the study and showcase the potential of the STA-based control method for DSIM applications.

In conclusion, this investigation introduces a significant advancement in DSIM control technology. The STA-based control method demonstrates superior speed control and efficiency, suggesting its potential for enhancing performance across a spectrum of industrial settings. The remainder of this paper is structured to provide a comprehensive exploration, including machine modeling, IFOC presentation, suggested structure, results, and a conclusive summary in Section 7.

## 2 DSIM Mathematical Models

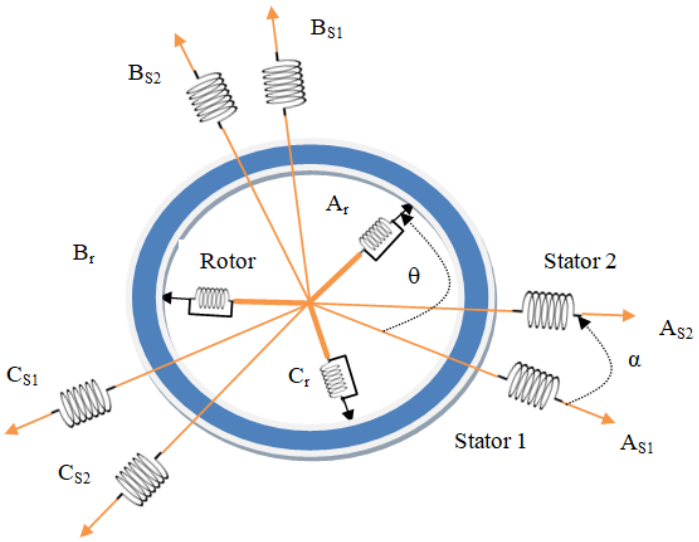


**Figure 1.** Representation of the DSIM winding

The mathematical model for the DSIM, represented by the simplified diagram in Figure 1, is provided by the following equations [8]:

$$\begin{cases} V_{ds1} = R_{s1} i_{ds1} + \frac{d}{dt}\phi_{ds1} - \omega_s \phi_{qs1} \\ V_{qs1} = R_{s1} i_{qs1} + \frac{d}{dt}\phi_{qs1} + \omega_s \phi_{ds1} \\ V_{ds2} = R_{s2} i_{ds2} + \frac{d}{dt}\phi_{ds2} - \omega_s \phi_{qs2} \\ V_{qs2} = R_{s2} i_{qs2} + \frac{d}{dt}\phi_{qs2} + \omega_s \phi_{ds2} \\ V_{dr} = 0 = R_r i_{dr} + \frac{d}{dt}\phi_{dr} - \omega_{gl} \phi_{qr} \\ V_{qr} = 0 = R_r i_{qr} + \frac{d}{dt}\phi_{qr} + \omega_{gl} \phi_{dr} \end{cases} \tag{1}$$

The rotor speed formulation is presented as follows:

$$J\frac{d\Omega}{dt} = T_{em} - T_L - F_r\Omega \tag{2}$$

The explanation of the torque $T_{em}$ is given below:

$$Tem = p\frac{L_m}{L_r + L_m}\left[\phi_{rd}\left(i_{qs1} + i_{qs2}\right) - \phi_{rq}\left(i_{ds1} + i_{ds2}\right)\right] \tag{3}$$

where the flux expressions are:

$$\begin{cases} \phi_{ds1} = L_{s1}i_{ds1} + L_m\left(i_{ds1} + i_{ds2} + i_{dr}\right) \\ \phi_{qs1} = L_{s1}i_{qs1} + L_m\left(i_{qs1} + i_{qs2} + i_{qr}\right) \\ \phi_{ds2} = L_{s2}i_{ds2} + L_m\left(i_{ds1} + i_{ds2} + i_{dr}\right) \\ \phi_{qs2} = L_{s2}i_{qs2} + L_m\left(i_{qs1} + i_{qs2} + i_{qr}\right) \\ \phi_{dr} = L_r i_{dr} + L_m\left(i_{ds1} + i_{ds2} + i_{dr}\right) \\ \phi_{qr} = L_r i_{qr} + L_m\left(i_{qs1} + i_{qs2} + i_{qr}\right) \end{cases} \tag{4}$$

## 3 DSIM Field-Oriented Control

The application of field-oriented control consists of the orientation of the rotor flux vector along the '$d$' axis, which can be expressed by considering $\phi_{\mathrm{dr}} = \phi_{\mathrm{r}}^*$ and $\phi_{\mathrm{qr}} = 0$. Consequently, the dynamic Eqs. (1), (2), and (3) after arrangement yield [2]:

The relation between torque and rotor flux is:

$$T_e^* = p\frac{L_m}{L_m + L_r}\left(i_{qs1} + i_{qs2}\right)\phi_r^* \tag{5}$$

The relation between slip speed and stator currents is:

$$\omega_{sl}^* = \frac{R_r}{L_m + L_r}\left(i_{qs1} + i_{qs2}\right) \tag{6}$$

Relations between voltages and currents components are:

$$\begin{cases} V_{ds1}^* = R_s i_{ds1} + sL_{s1}i_{ds1} - \omega_s^*\left(L_{s1}i_{qs1} + T_r\phi_r^*\omega_{sl}^*\right) \\ V_{qs1}^* = R_s i_{qs1} + sL_{s1}i_{qs1} + \omega_s^*\left(L_{s1}i_{ds1} + \phi_r^*\right) \\ V_{ds2}^* = R_s i_{ds2} + sL_{s2}i_{ds2} - \omega_s^*\left(L_{s2}i_{qs2} + T_r\phi_r^*\omega_{sl}^*\right) \\ V_{qs2}^* = R_s i_{qs2} + sL_{s2}i_{qs2} + \omega_s^*\left(L_{s2}i_{ds2} + \phi_r^*\right) \end{cases} \tag{7}$$

where, $T_r = \frac{l_r}{R_r}$ is the time rotor constant.

The voltage expressions show that the axes '$d-q$' are not independent, so, for a decoupling system, it's necessary to introduce new variables.

$$\begin{cases} V_{ds1-c} = \omega_s^*\left(L_{s1}i_{qs1} + T_r\phi_r^*\omega_{sl}^*\right) \\ V_{qs1-c} = \omega_s^*\left(L_{s1}i_{ds1} + \phi_r^*\right) \\ V_{ds2-c} = \omega_s^*\left(L_{s2}i_{qs2} + T_r\phi_r^*\omega_{sl}^*\right) \\ V_{qs2-c} = \omega_s^*\left(L_{s2}i_{ds2} + \phi_r^*\right) \end{cases} \tag{8}$$

and:

$$\begin{cases} V_{ds1} = R_s i_{ds1} + sL_{s1}i_{ds1} \\ V_{qs1} = R_s i_{qs1} + sL_{s1}i_{qs1} \\ V_{ds2} = R_s i_{ds2} + sL_{s2}i_{ds2} \\ V_{qs2} = R_s i_{qs2} + sL_{s2}i_{qs2} \end{cases} \tag{9}$$

The equation system (9) shows that stator voltages are directly related to stator currents. To compensate for the error introduced at decoupling time, the voltage references at constant flux are given by:

$$\begin{cases} V_{ds1}^* = V_{ds1} - V_{ds1-c} \\ V_{qs1}^* = V_{qs1} + V_{qs1-c} \\ V_{ds2}^* = V_{ds2} - V_{ds2-c} \\ V_{qs2}^* = V_{qs2} + V_{qs2-c} \end{cases} \tag{10}$$

For perfect decoupling, we add the loops that control the stator currents $i_{ds1}, i_{qs1}, i_{ds2}, i_{qs2}$ and get the stator voltages $V_{ds1}, V_{qs1}, V_{ds2}, V_{qs2}$ at their output. The field weakening block, which is characterized by a nonlinear function, normally keeps the flux constant at its nominal value. The IFOC uses a PWM source voltage inverter to supply the DSIM.

The DSIM schematic diagram with speed controller and IFOC technique is presented in Figure 2 in accordance with the analysis mentioned above.

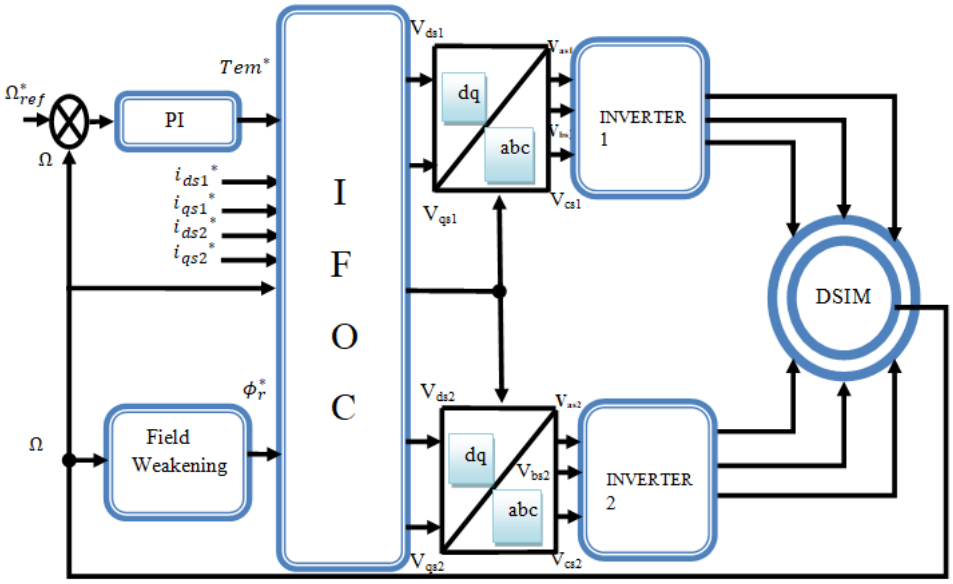


**Figure 2.** IFOC scheme for DSIM

## 4 STA

In the literature, several methods have been proposed to reduce or eliminate the chattering phenomenon, which is considered the primary drawback of the classical sliding mode controller [16, 17]. However, it is considered that the high-order sliding mode control (HOSMC) is one of the better solutions to reduce chattering and improve resilience during the convergence phase to the sliding surface compared to the conventional sliding mode control [18–20]. HOSMC versions use twisting, suboptimal, and STA. The STA method is commonly used because of its robustness, simplicity, ease of implementation, and easily adjustable response. Also, this method has been used in various areas, including electronics and machine control [21, 22]. The STA can be described by the following equation:

$$\begin{cases} U = \lambda 1 \sqrt{|e|}\,\mathrm{sign}(e) + U_1 \\ U_1 = \lambda 2 \cdot \mathrm{sign}(e) \end{cases} \tag{11}$$

where, $e$ is the error, $\lambda 1$ and $\lambda 2$ are positive coefficients.

Based on Eq. (11) and to simplify the understanding and working principle of the STA controller, Figure 3 is designed, in which a scheme of the working principle of the STA controller is presented.

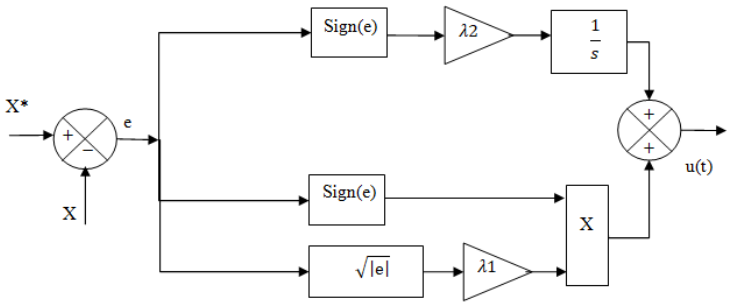


**Figure 3.** STA controller

## 5 STA Controller Design for IFOC of DSIM

The controller is used to regulate the speed and stator currents. The errors of the speed and stator currents are shown in Eqs. (11)-(15), respectively:

$$\mathrm{e}_\Omega = \Omega^*_{ref} - \Omega \tag{12}$$

$$e_{i_{ds1}} = {i_{ds1}}^* - i_{ds1} \tag{13}$$

$$e_{i_{ds2}} = {i_{ds2}}^* - i_{ds2} \tag{14}$$

$$e_{i_{qs1}} = {i_{qs1}}^* - i_{qs1} \tag{15}$$

$$e_{i_{qs2}} = {i_{qs2}}^* - i_{qs2} \tag{16}$$

These errors are used as inputs for the STA controller. The control law is designed to influence the torque and stator voltage components as presented in Eqs. (17)-(21) respectively.

$$\begin{cases} Tem^* = \lambda 1 \sqrt{|e_\Omega|} sign\left(e_\Omega\right) + Tem \\ Tem = \lambda 2 \cdot sign\left(e_\Omega\right) \end{cases} \tag{17}$$

$$\begin{cases} V_{ds1}^* = \lambda 1 \sqrt{|e_{i_{ds1}}|} sign\left(e_{i_{ds1}}\right) + V_{ds1} \\ V_{ds1} = \lambda 2 \cdot sign\left(e_{i_{ds1}}\right) \end{cases} \tag{18}$$

$$\begin{cases} V_{ds2}^* = \lambda 1 \sqrt{|e_{i_{ds2}}|} sign\left(e_{i_{ds2}}\right) + V_{ds2} \\ V_{ds2} = \lambda 2 \cdot sign\left(e_{i_{ds2}}\right) \end{cases} \tag{19}$$

$$\begin{cases} V_{qs1}^* = \lambda 1 \sqrt{|e_{i_{qs1}}|} sign\left(e_{i_{qs1}}\right) + V_{qs1} \\ V_{qs1} = \lambda 2 \cdot sign\left(e_{i_{qs1}}\right) \end{cases} \tag{20}$$

$$\begin{cases} V_{qs2}^* = \lambda 1 \sqrt{|e_{i_{qs2}}|} \operatorname{sign}\left(e_{i_{qs2}}\right) + V_{qs2} \\ V_{qs2} = \lambda 2 \cdot \operatorname{sign}\left(e_{i_{qs2}}\right) \end{cases} \tag{21}$$

The STA controllers for the speed and stator currents with the IFOC strategy are presented in Figures 4 and 5.

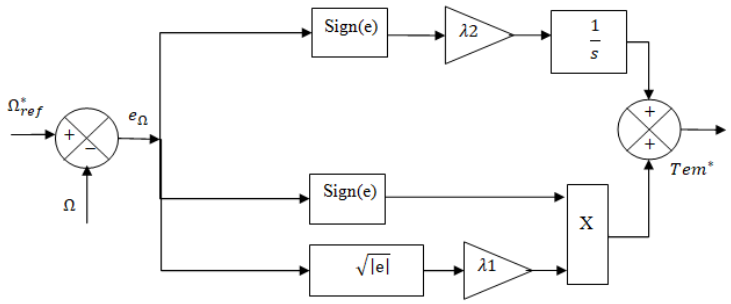


**Figure 4.** STA speed controller

The STA controllers are applied in an IFOC strategy to achieve accurate reference speed tracking, minimize torque ripple, reduce current ripple, and mitigate the chattering phenomenon. The IFOC-STA technique is illustrated in Figure 6.

## 6 Simulation Results and Discussion

The Matlab/Simulink software was used to implement the suggested STA controller for IFOC control of the DSIM. A comparison of speed, currents, and torque for trajectory tracking, as well as a robustness test between the proposed technique and the traditional PI controller, was conducted. The parameters of the DSIM used in the simulations are as follows:

$$\mathrm{P} = 4.5\ \mathrm{kW}; \mathrm{R_{s1}} = \mathrm{R_{s2}} = 3.72\Omega; \mathrm{R_r} = 2.12\Omega$$
$$\mathrm{L_{s1}} = \mathrm{L_{s2}} = 0.022\mathrm{H}; \mathrm{L_r} = 0.006\mathrm{H}; \mathrm{L_m} = 0.3672\mathrm{H};$$
$$\mathrm{p} = 1; \mathrm{J} = 0.0662\ \mathrm{kg \cdot m^2}; \mathrm{k_f} = 0.001\mathrm{Nm.s/rad}$$

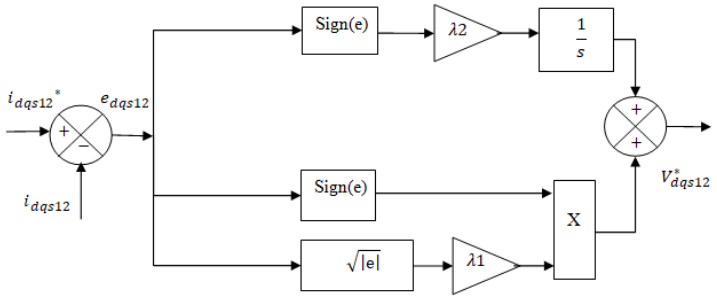


**Figure 5.** STA stator current $i_dqs12$ controller

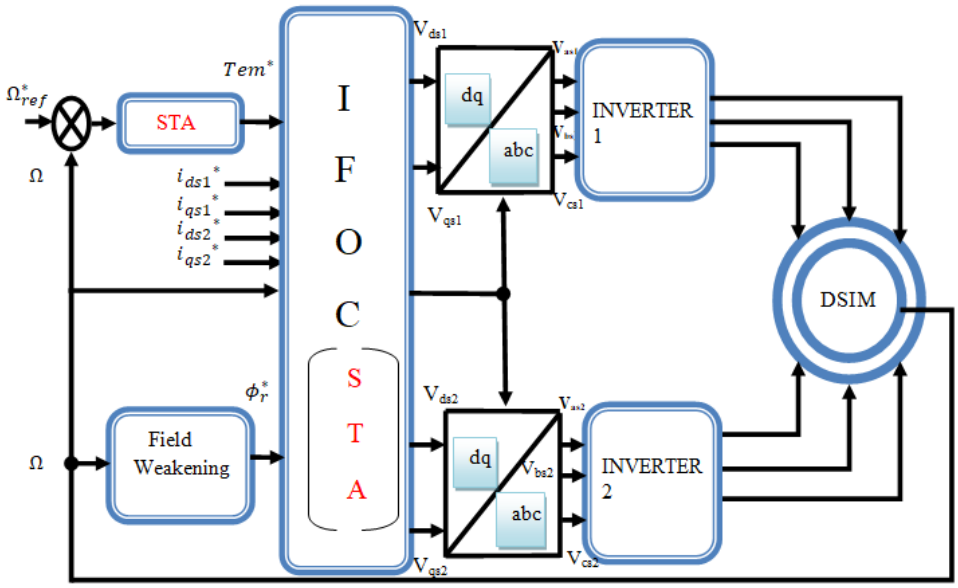


**Figure 6.** IFOC-STA control of DSIM

In Figures 7, 8, and 9, the speed, electromagnetic torque, and stator current of the systems are represented during a no-load start, with a load torque of 14 N.m. applied at t=0.8 s. In this test, where the command input is a speed step, it is clear that the tracking features of the response are better. The system quickly rejects the external disturbance. The proposed IFOC-STA technique has demonstrated fast reference tracking, ripple minimizing, and chattering phenomenon decreasing.

In the second test, the speed is switched at 2 s from 50 rad/s to 100 rad/s and after to 150 rad/s. We apply a load torque of 14 N.m. at time t = 1.5 s.

**Table 1.** Summary of the results obtained from the two strategiesf

| Criteria | Techniques | |
|---|---|---|
| | **IFOC-PI** | **IFOC-STA** |
| Rise Time (sec) | 0.1810 | 0.0752 |
| Settling Time (sec) | 0.1692 | 0.1140 |
| Overshoot (%) | 3% | 0.01% |
| Dynamic Response(sec) | Medium | Quick |
| Speed Tracking | Acceptable | Excellent |
| Steady State Error (%) | $> 1$ | Negligible |
| Torque Fluctuation Reduction | Medium | Very good |
| Minimization of Stator Current Ripple | Medium | Very good |
| Stator Current Quality | Acceptable | Good |

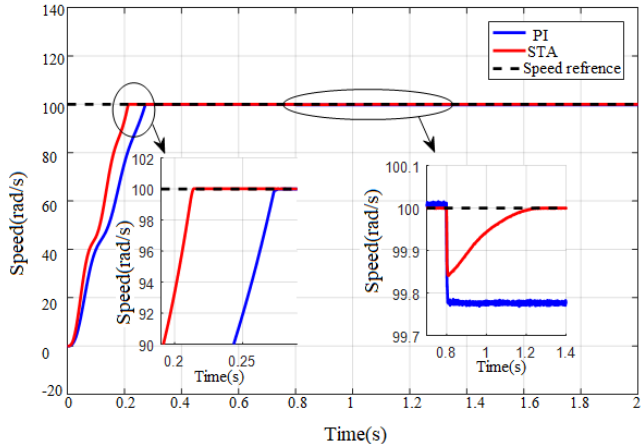


**Figure 7.** Speed of DSIM

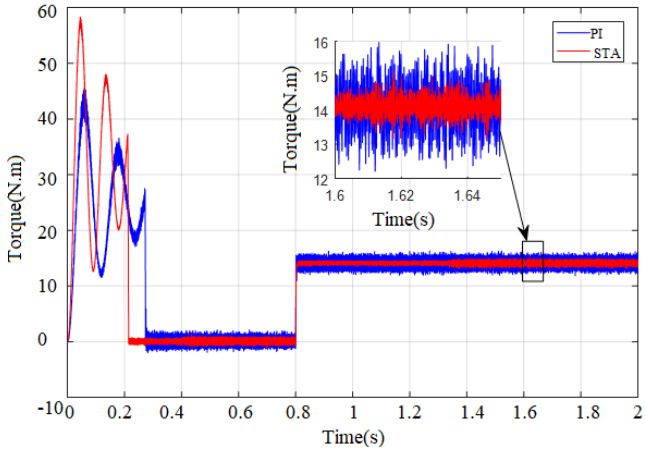


**Figure 8.** Torque of DSIM

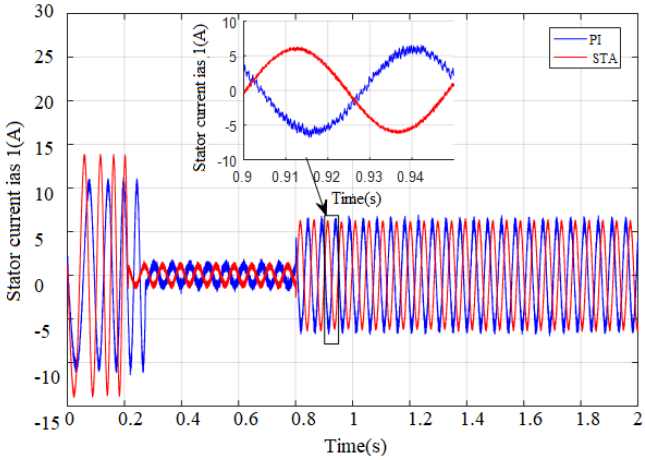


**Figure 9.** Stator current ias1

Figures 10, 11, and 12 demonstrate a fast response and efficacy in minimizing stator current and torque ripples. The proposed IFOC-STA strategy outperforms the IFOC-PI control strategy.

Table 1 provides a summary of the results and a comparison between the IFOC-PI technique and the proposed IFOC-STA method.

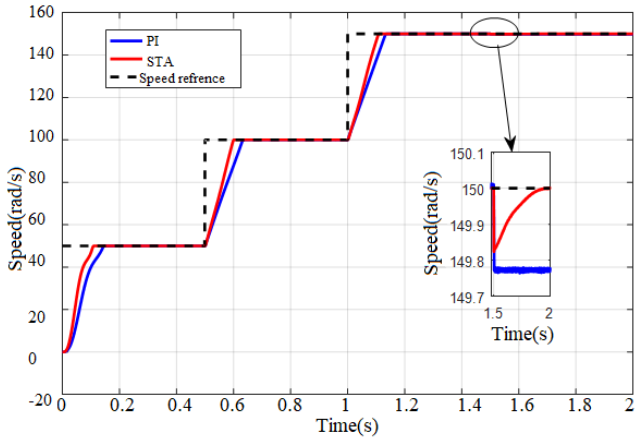


**Figure 10.** Speed response of the DSIM

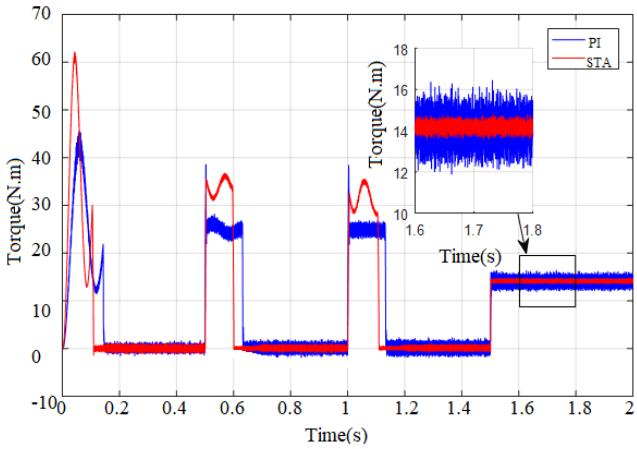


**Figure 11.** Torque of DSIM

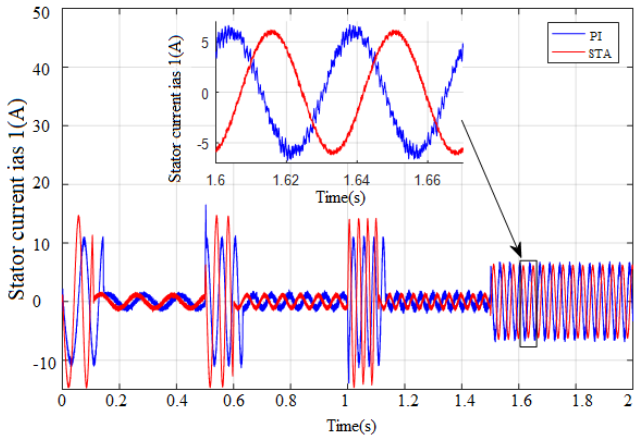


**Figure 12.** Stator current ias1

## 7 Conclusions

This study gave a comprehensive analysis of DSIM control, with a focus on the application of the STA as opposed to the conventional PI controller. It's observed that the STA-based control methodology markedly outperforms the traditional PI approach. Notable enhancements include a significant reduction in torque ripples, refined speed control, and superior disturbance rejection capabilities. Through rigorous simulation, the robustness and effectiveness of the

STA controller in mitigating the limitations associated with the PI controller had been convincingly demonstrated.

These findings contribute substantially to the field of DSIM control, providing essential insights for both researchers and practitioners specializing in electric variable speed drives. It is suggested that future research could explore the integration of the STA controller with a Fractional Order Proportional-Integral controller to further bolster resistance to disturbances. Additionally, the employment of multi-objective optimization methods to concurrently maximize several criteria, yielding a spectrum of Pareto-optimal solutions, presents an intriguing avenue for exploration. These solutions could then be selectively applied based on specific parameter requirements. Another prospective area of study involves the application of the proposed controller across various motor and system types, broadening the scope of its utility.

The expansion of these areas of research holds the potential to further refine DSIM control strategies, offering a wider range of adaptable and efficient solutions for varying industrial requirements. Consistent use of professional terms throughout the paper ensures a clear and comprehensive exposition of the subject matter, aligning with the high standards of top-tier academic journals.

## Data Availability

The data used to support the findings of this study are available from the corresponding author upon request.

## Conflicts of Interest

The authors declare that they have no conflicts of interest.

## References


[1] E. Terfia, S. Rezgui, S. Mendaci, H. Gasmi, and H. Benalla, "Optimal fractional order proportional integral controller for dual star induction motor based on particle swarm optimization algorithm," *J. Eur. Syst. Autom.*, vol. 56, no. 2, pp. 345–353, 2023. https://doi.org/10.18280/jesa.560220

[2] S. Lekhchine, T. Bahi, and Y. Soufi, "Indirect rotor field oriented control based on fuzzy logic controlled double star induction machine," *Int. J. Electr. Power Energy Syst.*, vol. 57, pp. 206–211, 2014. https://doi.org/10.1016/j.ijepes.2013.11.053

[3] H. Rahali, S. Zeghiache, and L. Benalia, "Adaptive field-oriented control using supervisory type-2 fuzzy control for dual star induction machine," *Parameters*, vol. 10, no. 4, pp. 28–40, 2017. https://doi.org/10.22266/ijies2017.0831.04

[4] K. Hamitouche, S. Chekkal, H. Amimeur, and D. Aouzellag, "A new control strategy of dual stator induction generator with power regulation," *J. Eur. Syst. Autom.*, vol. 53, no. 4, pp. 469–478, 2020. https://doi.org/10.18280/jesa.530404

[5] L. Bentouhamia, R. Abdessemedb, A. Kessala, and E. Merabeta, "Control neuro-fuzzy of a dual star induction machine (DSIM) supplied by five-level inverter," *J. Power Technol.*, vol. 98, no. 1, pp. 70–79, 2018.

[6] N. Layadi, A. Houari, S. Zeghlache, M. F. Benkhoris, A. Djerioui, and F. Berrabah, "Integral backstepping control for double star induction machine (DSIM)," in *2018 Int. Conf. Electr. Sci. Technol. Maghreb (CISTEM), Algiers, Algeria*, 2018, pp. 1–6. https://doi.org/10.1109/CISTEM.2018.8613328

[7] A. Oumar, Y. Ahmed, and M. Cherkaoui, "Operating of DSIM without current and speed sensors controlled by ADRC control," *Math. Probl. Eng.*, vol. 2022, 2022. https://doi.org/10.1155/2022/9033780

[8] G. Boukhalfa, S. Belkacem, A. Chikhi, and S. Benaggoune, "Direct torque control of dual star induction motor using a fuzzy-PSO hybrid approach," *Appl. Comput. Inform.*, vol. 18, no. 1/2, pp. 74–89, 2022. https://doi.org/10.1016/j.aci.2018.09.001

[9] R. Sadouni and A. Meroufel, "Indirect rotor field-oriented control (IRFOC) of a dual star induction machine (DSIM) using a fuzzy controller," *Acta Polytech. Hung.*, vol. 9, no. 4, pp. 177–192, 2012.

[10] C. Hadji, D. Khodja, and S. Chakroune, "Robust adaptive control of dual star asynchronous machine by reference model based on landau stability theorem," *Adv. Model. Anal. C*, vol. 74, no. 2-4, pp. 56–62, 2019. https://doi.org/10.18280/ama_c.742-403

[11] K. Sahraoui, K. Kouzi, and A. Ameur, "Optimization of MRAS based speed estimation for speed sensorless control of DSIM via genetic algorithm," *Electroteh. Electron. Autom.*, vol. 65, no. 3, pp. 157–162, 2017.

[12] A. Benamor, M. T. Benchouia, K. Srairi, and M. E. H. Benbouzid, "A novel rooted tree optimization apply in the high order sliding mode control using super-twisting algorithm based on DTC scheme for DFIG," *Int. J. Electr. Power Energy Syst.*, vol. 108, pp. 293–302, 2019. https://doi.org/10.1016/j.ijepes.2019.01.009

[13] L. Xiong, P. Li, F. Wu, M. Ma, M. W. Khan, and J. Wang, "A coordinated high-order sliding mode control of DFIG wind turbine for power optimization and grid synchronization," *Int. J. Electr. Power Energy Syst.*, vol. 105, pp. 679–689, 2019. https://doi.org/10.1016/j.ijepes.2018.09.008

[14] L. Laggoun, L. Youb, S. Belkacem, S. Benaggoune, and A. Craciunescu, "Direct torque control using second order sliding mode of a double star permanent magnet synchronous machine," *UPB Sci. Bull. Ser. C*, vol. 80, no. 4, pp. 93–106, 2018.

[15] B. Kiyyour, D. Naimi, A. Salhi, and L. Laggoune, "Hybrid fuzzy second-order sliding mode control speed for direct torque control of dual star induction motor," *J. Fundam. Appl. Sci.*, vol. 11, no. 3, pp. 1440–1454, 2019.

[16] H. O. Ozer, Y. Hacioglu, and N. Yagiz, "High order sliding mode control with estimation for vehicle active suspensions," *Trans. Inst. Meas. Control*, vol. 40, no. 5, pp. 1457–1470, 2018. https://doi.org/10.1177/0142331216685394

[17] H. Gasmi, S. Mendaci, S. Laifa, W. Kantas, and H. Benbouhenni, "Fractional-order proportional-integral super twisting sliding mode controller for wind energy conversion system equipped with doubly fed induction generator," *J. Power Electron.*, vol. 22, no. 8, pp. 1357–1373, 2022. https://doi.org/10.1007/s43236-022-00430-0

[18] C. Hadji, D. Khodja, and S. Chakroune, "Robust adaptive control of dual star asynchronous machine by reference model based on landau stability theorem," *Adv. Model. Anal. C*, vol. 74, no. 2-4, pp. 56–62, 2019. https://doi.org/10.18280/ama_c.742-403

[19] H. Chaabane, K. D. Eddine, and C. Salim, "Indirect self tuning adaptive control of double stars induction machine by sliding mode," *Rev. Roum. Sci. Tech.-Electrotech. Energ.*, vol. 64, no. 4, pp. 409–415, 2019.

[20] Y. Shtessel, M. Taleb, and F. Plestan, "A novel adaptive-gain supertwisting sliding mode controller: Methodology and application," *Automatica*, vol. 48, no. 5, pp. 759–769, 2012. https://doi.org/10.1016/j.automatica.2012.02.024

[21] G. V. Hollweg, P. J. D. de Oliveira Evald, D. M. C. Milbradt, R. V. Tambara, and H. A. Gründling, "Design of continuous-time model reference adaptive and super-twisting sliding mode controller," *Math. Comput. Simul.*, vol. 201, pp. 215–238, 2022. https://doi.org/10.1016/j.matcom.2022.05.014

[22] K. Walid, M. Sofiane, H. Benbouhenni, G. Hamza, and T. Es-saadi, "Application of third-order sliding mode controller to improve the maximum power point for the photovoltaic system," *Energy Rep.*, vol. 9, pp. 5372–5383, 2023. https://doi.org/10.1016/j.egyr.2023.04.366

**Nomenclature**

| | |
|---|---|
| $\boldsymbol{s}$ | Stator |
| $\boldsymbol{r}$ | Rotor |
| $\boldsymbol{V}_{ds1}, \boldsymbol{V}_{qs1}, \boldsymbol{V}_{ds2}, \boldsymbol{V}_{qs2}$ | Voltages in the d-q axis for stator 1 and 2 |
| $\boldsymbol{I}_{ds1}, \boldsymbol{I}_{qs1}, \boldsymbol{I}_{ds2}, \boldsymbol{I}_{qs2}$ | Currents in the d-q axis for stator 1 and 2 |
| $I_{dr}, I_{qr}$ | Rotor currents d-q axis |
| $\boldsymbol{\Phi}_{ds1}, \boldsymbol{\Phi}_{qs1}, \boldsymbol{\Phi}_{ds2}, \boldsymbol{\Phi}_{qs2}$ | Stator flux vectors d-q axis components |
| $\Phi_{dr}, \Phi_{qr}$ | Rotor flux vectors d-q axis components |
| $\boldsymbol{T}_{em}$ | Electromagnetic torque |
| $\boldsymbol{T}_{L}$ | Load torque |
| $\boldsymbol{\Omega}_{r}$ | Mechanical speed |
| $\boldsymbol{\Omega}_{ref}$ | Reference Mechanical speed |
| $\omega_r$ | Angular speed for rotor |
| $\omega_s$ | Angular speed for stator |
| $\boldsymbol{P}$ | Number of pole pairs |
| $\boldsymbol{J}$ | Moment of Inertia |
| $\boldsymbol{F_r}$ | Friction coefficient |
| $\boldsymbol{R}_{s1}, \boldsymbol{R}_{s2}$ | resistances in Stator |
| $\boldsymbol{R}_{r}$ | resistances in Rotor |
| $\boldsymbol{L}_{s1}, \boldsymbol{L}_{s2}$ | self-inductances in Stator |
| $\boldsymbol{L}_{m}$ | Cyclic mutual inductance |
| $\boldsymbol{L}_{r}$ | Self-inductances in Rotor |